MASTER

GAMMA-RAYS FROM DEEP INELASTIC COLLISIONS*

F. S. Stephens

Lawrence Berkeley Laboratory
University of California
Berkeley, California 94720

Summary

The γ-rays associated with deep inelastic collisions can give information about the magnitude and orientation of the angular momentum transferred in these events. In this review, special emphasis has been placed on understanding the origin and nature of these γ-rays in order to avoid some of the ambiguities that can arise. The experimental information coming from these γ-ray studies is reviewed, and compared briefly with that obtained by other methods and also with the expectations from current models for deep inelastic collisions.

DISCLAIMER

[illegible]

* This work was supported by the Nuclear Physics Division of the U. S. Department of Energy under contract No. W-7405-ENG-48.

DISTRIBUTION OF THIS DOCUMENT IS UNLIMITED

I. Introduction

My objective in this talk is to consider the question: "What can be learned about deep inelastic collisions (DIC) from studying the associated gamma rays?" It is a somewhat difficult subject, with a number of uncertainties and ambiguities. This has led some people to conclude that the answer to this question is "nothing." I hope to convince you otherwise. First, I want to discuss the origin and nature of the gamma rays from DIC, then the kinds of information gamma-ray spectra contain, and finally come to the combination of these two subjects.

II. The Gamma Rays from DIC

In Fig 1 I have sketched the excitation energy of a DIC product nucleus vs angular momentum. This figure is made for a mass number around 160, although the general consideration to be made do not depend very strongly on mass number. The first feature to notice in Fig. 1 is that above a certain angular momentum (~70ħ for A ~ 160) the product nucleus fissions,[1] resulting in two lighter product nuclei at much lower angular momentum. Below this critical angular momentum (which comes when the fission barrier is around 8 MeV), particle evaporation dominates over fission, deexciting the nucleus toward its ground state (i.e., that of the appropriate neighboring nucleus). If this evaporation is mostly neutrons, which tends to be the case for high-Z, and/or neutron-rich systems, then very little angular momentum is lost in the process ($\lesssim$1ħ per neutron). However, charged particles, especially α particles, can remove large amounts of angular momentum--up to 20ħ per α particle. The particle evaporation process proceeds to the so-called "entry line," a region about 8 or 10 MeV above the yrast line, from which point γ-ray deexcition dominates. (The yrast line is the line below which no states exist for that angular momentum.) Thus, the γ-rays dominate only below the point where a particle binding energy is no longer available without a significant reduction of angular momentum.

The deexcitation γ-rays are divided into two types--resolved and unresolved--depending on whether enough population goes through a given transition to make it stand up in the spectrum, or not. In

general the resolved transitions occur only near the bottom of the cascade, i.e., for $I \lesssim 10\hbar$. The unresolved transitions are further divided into two types, those that carry off angular momentum (yrast-like) and those that cool the nucleus without carrying much angular momentum (statistical). In Fig. 1, four statistical transitions are indicated, which is typical, and the last 5 or 6 yrast-like transitions would probably have sufficient population to be resolved in the spectrum. Above this spin, there are hundreds or even thousands for pathways (one of which is indicated), and nothing is resolved in the spectrum, giving rise to the so called "continum." It is apparent from Fig. 1 that the <u>number</u> of γ-rays gives information about the initial angular momentum in the product nucleus. To interpret this information we must know (1) how much angular momentum has been lost during the particle evaporation, and (2) the nature of the γ-rays emitted. A discussion of these topics will come somewhat later, however it is essential from the outset to realize that most of our information about the nature of the γ-rays involved in DIC comes from studies of the deexcitation of compound nuclei following heavy-ion fusion reactions. It is important to understand why we believe this information is relevant.

A diagram like Fig. 1 for the product of a compound-nucleus reaction would look very similar except that the initial excitation energy is constant but can be varied--it is in general adjusted (by the bombarding energy) to be much lower than 100 MeV (usually 50-60 MeV). This results in fewer particles evaporated, but

presumably in no change to the decay from a given point on or near the entry line. This is because the entry line, yrast line, and fission barrier, are nuclear properties and are not expected to depend on how that nucleus is formed. It would be very exciting if some information about the entrance channel survived to the entry line, but this seems highly unlikely and there is no evidence at present to suggest it. Thus we should be able to apply our information about compound-nuclear γ-rays to product nuclei from DIC. The outline of the decay process given above comes from this source.

A spectrum of γ-rays from a compound nucleus reaction[2] is shown in Fig. 2. Two features are apparent and seem to be general. The statistical transitions fall off exponentially with increasing γ-ray energy above ~2 MeV and are currently thought to follow an intensity relationship something like:

$$N_\gamma = kE_\gamma^2 e^{-E_\gamma/T} \tag{1}$$

where T is a temperature around 1 MeV, and k is adjusted so that the integral over E_γ is 3 or 4 transitions. The yrast-like γ-rays are the most important for the present discussion, since they carry off the angular momentum. They comprise a "bump" in the γ-ray spectrum that lies below about 2 MeV as is seen in Fig. 2. Their nature is sensitive to the nuclear structure, ranging from predominantly stretched quadrupole transitions ($I \rightarrow I-2$) in regions of rotational nuclei, to mixtures containing 50 percent or more of dipole

transitions in other regions. Unfortunately the non-rotational regions are the most common and in these cases our knowledge of individual nuclei is generally rather poor.

III. Information Content of γ-Ray Spectra

Before beginning a detailed discussion of γ-rays from DIC, it seems useful to consider briefly what one can possibly learn from γ-ray studies, and why only two types of studies will be discussed here in connection with DIC. I will list and make a few comments on the types of measurements commonly made to study γ-rays. First (1) one can measure the total γ-ray energy; the sum of all individual γ-ray energies for a given reaction. This has not yet been done for DIC, though it is very likely imminent. It is obviously important for the total energy balance in the reaction, though Fig. 1 shows that γ-ray energy is not a large component in that balance. Perhaps more important, it is related to the angular momentum. Figure 1 shows that at $40\hbar$, an extra 10 MeV appears as γ-ray energy, and at $60\hbar$, 20 MeV. This is potentially a sensitive way to measure these angular momenta, which is independent of transition type. Next (2) one can measure individual γ-ray energies. These are related to the nuclear structure, and can be used, for example, to identify a reaction product. If their multipole character is known, they can be used to determine the alignment of the angular momentum in the product nucleus emitting them. Then (3) we can measure the angular distribution of the emitted γ-rays for the purpose (here) of defining the angular momentum axis of the system. This subject will be one of two main topics discussed. Further, (4) the polarization of the γ-radiation can be measured. This can serve to define not only the axis of the angular momentum,

but also its direction. Professor J. de Boer will discuss this topic later in the school, so I will not take it up. An important property (5) to measure is the total number of γ-rays emitted, the multiplicity. This is obviously related to the total angular momentum and will be the other main topic discussed here. Finally (6) the time of γ-ray emission can be measured. These are generally in the range 10^{-14}-10^{-9} sec after the reaction, and this is much too late to give information about the time development of DIC. So far, these times have been used mainly to relate the γ-rays to particular events (selected in other detectors). As mentioned, I will discuss only two of these areas, the multiplicities and the angular distributions.

IV. Gamma-Rays from DIC

1. Multiplicities

We want to measure multiplicity to relate it to the spin transferred to the internal degrees of freedom of the product nuclei. As mentioned earlier, we must first determine how much angular momentum is carried off by the particle evaporation. Natowitz[3] has made a systematic attempt to relate multiplicity to spin for different-mass product nuclei, and his plot is shown in Fig. 3. Two features are apparent. The top of the plot, A ~ 150, is in the rare earth region of rotational nuclei, and a good approximation there is the emission of four statistical γ-rays (carrying no angular momentum) and the rest stretched E2 transitions. Then the spin is related to multiplicity by:

$$I = 2(M_\gamma - 4) \quad , \tag{2}$$

as has been suggested in numerous compound-nucleus studies. On the other hand, near the bottom of Fig. 3, A $\lesssim$ 50, the (charged) particle evaporation has carried off essentially all the angular momentum, so that the deexcitation involves only 3-4 transitions, irrespective of initial spin. This total lack of sensitivity of the multiplicity to spin for light nuclei is not without some benefit (as might first appear), since for a reaction with a heavy and a light product, the contribution of the light product can be simply <u>assumed</u> to be 3 or 4 γ-rays, enabling one to deduce the spin of the heavy product. Between these mass limits the particle evaporation removes part, but not all of the angular momentum, and the situation is more complex.

While I am very sympathetic to the kind of systematic approach taken by Natowitz, one must be very careful. At least three more dimensions are needed in Fig. 3. The first is the relation of the product nucleus to beta stability. The evaporation ratio of neutrons to charged particles is sensitive to the respective binding energies, which is a strong function of neutron to proton ratio. Thus even at $A \gtrsim 150$, if one goes sufficiently far neutron deficient, charged particles will be evaporated and they will carry angular momentum. Conversely, if one goes as low as $A \sim 110$, but stays very neutron rich, then neutron evaporation still predominates and carrys little angular momentum. A second dimension to add to Fig. 3 is excitation energy. This will not matter so much near the top or bottom of Fig. 3, where, respectively, "very little" or "all" of the angular momentum is removed by the evaporation cascade; but it must be important in the middle region where just part of the angular momentum has been removed. A longer cascade will surely remove more in that case. The final dimension to add to Fig. 3 is for type of γ-ray emitted, as discussed earlier in connection with Fig. 2. We will look now in slightly more detail, at just how an uncertainty in the type of γ-ray emitted affects the spin deduced.

From studies of compound-nucleus γ-ray, we know that the deexcitation is generally fast ($\lesssim 10^{-9}$ sec); the occurrance of longer-lived isomers involving more than one or two γ-rays is not common. This lifetime limit restricts the transition types to dipole and quadrupole. If high or moderately high spins are involved, the

level densities strongly favor "stretched" transitions, i.e., those that maximize the reduction of angular momentum ($I \rightarrow I-1$ for dipoles and $I \rightarrow I-2$ for quadrupoles). On the assumption of just these two types, we can use the angular anisotropy of the emitted γ-rays to determine how much there is of each type. Figure 4 shows some results from a recent compound-nucleus study.[4] In the region of rotational nuclei ($90 \lesssim N \lesssim 110$) one finds 80 percent stretched E2 transitions, roughly consistent with Eq. 2. But below that region there is a wide variation down to as low as 30 percent. There are certainly strong nuclear structure effects in these variations--the highest stretched E2 intensities coming for the rotational nuclei, and the lowest in Fig. 4 at the 82 neutron closed shell. Figure 4 also shows that these values do not depend (much, at least) on the projectile involved. While there are assumptions involved in obtaining these numbers, so that they might be wrong in particular cases (or even in general at low spin values) it seems rather safe to take them as representative of the types of γ-rays we are likely to encounter in DIC studies. In order to get spins from multiplicities, assuming stretched transitions, one has simply:

$$I_\gamma = M_\gamma(1 + Q/(Q+D)) \quad , \tag{3}$$

where Q and D are the amounts of stretched quadrupole and dipole transitions, respectively. The full range shown on Fig. 4 then corresponds to : $1.3 \lesssim I_\gamma/M_\gamma \lesssim 1.8$, so that, $I_\gamma/M_\gamma \sim 1.6$,

should generally be correct within about 20 percent. Higher accuracy is probably hard to achieve except for rotational nuclei, and even this kind of accuracy will be valid only for moderately high initial spins. Thus for determining spins from multiplicities, the nature of the particle evaporation generally causes greater uncertainties than does the nature of the γ-rays emitted.

The general features of γ-ray multiplcities associated with DIC were measured by Berlanger et al,[5] and are shown in Fig. 5. The system studied was 443 MeV Cu on Au, at a particle angle of 35° to the beam direction. One sees a very low multiplicity for the elastic events, sharply rising in the quasielastic region, and high (~20) throughout the strongly inelastic region. In general, this demonstrates the transfer of angular momentum, along with energy, into the internal degrees of freedom of the products of the DIC events. Since this measurement a number of studies have been made, and the results differ according to whether the system is "light" (sufficiently low total Z so that there is considerable fusion) or "heavy" (high enough total Z so that no fusion can occur). Both of these limits will be considered.

A simple model against which the observed distribution of angular momenta in DIC can be compared is that of two spheres (or spheroids) sticking together and rotating rigidly (no rolling or sliding) prior to breakup—the socalled "sticking limit." In such a model, the amount of angular momentum transferred to the internal degrees of freedom, Δl, depends on the moments of inertia according to the relationship:

$$\Delta l = l_i - l_f = l_i\left(\frac{\mathcal{J}_L + \mathcal{J}_H}{\mathcal{J}_L + \mathcal{J}_H + \mathcal{J}}\right) \tag{4}$$

where l_i is the initial angular momentum of the system and $\mathcal{J}_L$ and $\mathcal{J}_H$ are the moments of inertia of the light and heavy fragments as given by $\mathcal{J}_i = 2/5\ A_i R_i^2$, and $\mathcal{J}$ is the moment of inertia of two spheres sticking at their point of contact, $\mathcal{J} = \mu(R_L + R_H)^2$. One sees that Δl varies from 2/7 of l_i when the fragments are equal, to l_i when the mass of the light fragment goes to zero (the compound-nucleus limit). The sticking limit was first shown by Glassel et al.[6] to be reached for the system ^{nat}Ag + (175 MeV) ^{20}Ne. Figure 6 shows that at angles backward of the grazing angle (90°) the shape of the multiplicity curve with Z_L is characteristic of the sticking limit; whereas around (and forward of) the gra ing angle this is not true. An even more convincing fit is shown in Fig. 7 due to Natowitz et al.[7] for the system ^{89}Y + (237 MeV) ^{40}Ar. In both cases there is some question as to whether the absolute multiplicity (implied Δl) is high enough to agree with Eq. (4) (possible reductions due to: (1) incomplete l-transfer; (2) l-fractionation; and (3) deformation have been discussed), but the general evidence for sticking seems rather strong in these systems. It should be noted that this agreement comes when: (1) there is a rather narrow l-range populated (fusion takes the lowest ~60ħ and the reactions bring in only ~70-90ħ); and (2) the times are long enough for the angular momentum to equilibrate (for these light systems the sticking time is very likely correlated to the scattering angle, and

the angles backward of grazing imply times long enough to rotate through 0° and then on to the measured angle).

When one goes to the heavy (high-Z) systems where there is little or no fusion, then neither of the above conditions is fulfilled. Essentially all l-waves now go into DIC events, so that the possibility of fractionation arises (i.e., a higher probability for certain l-values to go into certain channels) and all interaction times tend to be short. Furthermore, scattering angle (or deflection function) is no longer found to be simply correlated to interaction times; in fact, there often tends to be a focussing effect of many different l-waves into the same scattering angle. In these cases, the multiplicities are rather independent of mass asymmetry for DIC events, as shown in Fig. 8 for two systems:[8] 618 MeV ^{86}Kr on ^{165}Ho and ^{nat}Ag. Other data are rather similar, and this behavior has been explained as due to rigid rotation modified by: (1) potential-energy surfaces which favor mass symmetry for high l-waves; and (2) interaction-time effects which correlate lower l-waves with greater distance (in mass asymmetry) from the entrance channel. The quasi-elastic (incomplete energy relaxation) events in Fig. 8 show a dip in multiplicity at the projectile mass. This presumably reflects decreasing l-transfer associated with the decreasing energy transfer, both due to very short average interaction times for these products which "remember" the entrance-channel.

Since for these heavy systems, the scattering angle is no longer connected simply to interaction time, another measurable indicator of this time is needed, and total kinetic energy loss is perhaps the most

promising possibility. Figure 9 shows the multiplicity for three systems[8] plotted against total (remaining) kinetic energy. One sees that the angular momentum transfer occurs over a particular range of energy transfers, and then is constant for still greater energy loss. The behavior of these multiplicities has been accounted for reasonably well by both classical dynamical models and by transport models. For the very large energy transfers (low l-waves) fluctuations in the transferred angular momentum have been suggested[11] to play a role.

If more than one γ-ray detector is used, higher moments of the multiplicity distribution can be measured. Ideally one would like to have a 4π γ-ray detector divided into many sectors and measure the exact multiplicity for each event. Then, after a number of events, a distribution like that at the top of Fig. 10a would result. Since the appropriate 4π detectors do not yet exist, we have to resort to measuring <u>average</u> moments of this distribution. So far we have discussed the average value (or first moment), which is called the multiplicity (middle of Fig. 10a). At the bottom of Fig. 10a the distribution is represented as a gaussian and the first and second moments (width or σ) are indicated. Third moments (skewness) have been measured in a few cases, but are still somewhat tentative. To give some feeling for these moments, Fig. 10b shows the triangular distribution characteristic of angular momentum input if all l-values up to a maximum value contribute. If the multiplicity is proportional to l, then the measured moments will be: an average multiplicity which

is 2/3 of the maximum value, a width such that $\sigma/\langle M \rangle = 0.35$, and a skewness of -0.57.

Several groups have measured widths from multiplicity distributions for DIC events.[9,10,12] The results of Dayras et al.[12] are shown in the top section of Fig. 11. Values of σ_γ/M_γ range around 0.45, even larger than that expected if the full distribution of l-values contribute, as discussed in connection with Fig. 10b. Other results are similar, and seem to require the introduction of sizeable fluctuations[11] in the transferred angular momentum. The transport models of DIC seem able to account for the fluctuations, which can also be introduced as bending, etc., modes into the classical dynamical models.[13] This subject will be further discussed in connection with angular distributions in the next section.

2. Angular Distributions

There is also an alignment of the angular momentum in a DIC. In the left part of Fig. 12 a typical arrangement of beam, target, and particle detectors is indicated. The reaction plane is thus defined to be the XZ plane. The angular momentum is aligned perpendicular to this plane, along the Y axis. The γ-rays following the DIC are then emitted anisotropically according to their character. The patterns for stretched quadrupole and dipole radiation are shown in the center and right portions of Fig. 12. We have argued that these two types are likely to dominate, though non-stretched transitions, as well as mixtures are possible. If stretched quadrupole transitions dominate, as is expected in some cases, then there will be very little radiation

perpendicular to the reaction plane. Conversly, a mixture of 60 percent stretched dipole and 40 percent stretched quadrupole is nearly isotropic. Here, the particle evaporation steps are not usually so important, but information about the nature of the γ-rays is absolutely essential. Measurements have been made on resolved and or unresolved γ-rays following DIC, and both will be discussed.

Gamma-rays have so far been resolved following DIC only in light systems. The first measurement by Van Bibber et al.[14] was for $^{16}O + ^{27}Al$, and γ-rays from ^{12}C, ^{22}Ne, ^{24}Mg and ^{31}P were observed in the Q-value range down to Q = -50 MeV. The results in Fig. 13 show essentially the full alignment expected at small Q values, with some evidence for reduced anisotropies at larger (negative) Q values. For the low spins involved here, however, this reduction might be due to dealignment during the preceeding (particle or γ-ray) decay process. Higher spins are involved in another study by Puchta et al.[15] on the system, $^{16}O + ^{48}Ti$. Their results in Fig. 14 show several interesting features. One sees first that the unresolved γ-spectrum is isotropic, most probably indicating mixtures of transition types. The γ-rays of ^{50}Cr are seen to develop a very strong anisotropy for Q values around -30 MeV, falling on either side of that. The low anisotropies for small Q values (~-20 MeV) the authors ascribe to low initial spin values with subsequent dealignment prior to emission of the observed γ-rays. The fall off toward larger negative Q values is taken as evidence for fluctuations in the spin axis with increasing inelasticity. It is interesting that the

anisotropy is nearly gone by $Q \lesssim -50$ MeV. The lower anisotropies for ^{46}Ti are ascribed by the authors to dealignment effects in the deexcitation cascade, as evidenced by the much larger side-feeding into the low-lying lower spin states of ^{46}Ti. This possibility of dealignment seems consistent with the high probability of spin removal in the particle and early γ-ray cascades in the very light systems (see Fig. 3). The ^{50}Cr product nucleus preserves both its spin and alignment (in part) because it is made largely by the $^{48}Ti(^{16}O,^{12}C)^{52}Cr^*$ reaction followed by evaporation of two neutrons from the $^{52}Cr^*$. These neutrons are not so efficient at carrying angular momentum as α particles. Figure 14b shows the behavior of P_{ZZ}, the alignment parameter defined as:

$$P_{ZZ} = \frac{3}{2}\left(\frac{I_Z^2}{I^2}\right) - \frac{1}{2} \quad . \tag{5}$$

The alignment is nearly complete around $Q \approx -30$ MeV, and drops to about 50 percent at $Q \approx -50$ MeV. Finally, Fig. 14c just shows the build-up of angular momentum into the ^{52}Cr system as estimated from the side-feeding patterns of the low-lying high-spin states of ^{50}Cr. These results are quite interesting as they suggest that the expected alignment may be strongly affected by fluctuations or other effects that set in at modestly small Q values.

The observed in-plane, out-of-plane anisotropy of the unresolved γ-rays following DIC have always been small--$\lesssim$25 percent. This applies to the very early Orsay work,[5] and, for example, to the

$^{20}Ne + ^{63}Cu$ work of Dayras et al.[12] (see the bottom section of Fig. 11). It has not been clear how to interpret these results. Because heavy systems and high spins have been involved in at least some cases, this is probably not due to dealignment effects in the deexcitation cascade. However, it might be due either to primary misalignment of the fragment angular momentum (due to fluctuations, etc., in the DIC), or to mixtures of γ-ray transition types (see Fig. 12). This has been a difficult question to resolve, since heavy mixtures of dipole and quadrupole transitions might be expected (Fig. 4). Perhaps the most convincing answer to this problem has been given by the measurement of Aguer et al.[16]

Aguer et al. studied the symmetric products ($A \sim 160$) from the reaction, 1064 MeV $^{136}Xe + ^{197}Au$. These products are sufficiently heavy and neutron rich to avoid charged particle evaporation (involving angular momentum and alignment loss) and are in the rare-earth region of rotational nuclei. It was verified that the multiplicity was very high (~40), roughly consistent with the high expected spin values of each fragment, and that the γ-ray spectra contained the characteristic "bump" of yrast-like γ-rays, which in this region are mainly rotational stretched quadrupole transitions. The anisotropy, both in-plane and out-of-plane, was measured and is shown in Fig. 15. The in-plane distribution is isotropic within the uncertainties, whereas in the E2-bump region ($E_\gamma \lesssim 1.5$ MeV) the ratio ($90^\circ_{out}/90^\circ_{in}$) is 0.75 ± 0.1. This small anisotropy for nearly pure ($\gtrsim$80 percent) stretched quadrupole transitions implies

substantial misalignment of the fragment angular momenta. The authors evaluate σ to be $34^\circ \pm 7^\circ$ in the expression for the probability $P(\theta)$ for alignment of the angular momentum around the vertical ($\theta = 0$):

$$P(\theta) \propto e^{-(\theta^2/2\sigma^2)} \quad . \tag{6}$$

This corresponds to a P_{ZZ} of 0.53 ± 0.17. This misalignment they attribute to bending and twisting classical modes, but it is probably equivalent to understand it as fluctuations in a transport model of DIC. The Q-value dependence perhaps suggests larger anisotropies for smaller Q values, but that is not clear from these data. This work suggests that alignment information can come from studying the unresolved γ-ray spectrum following DIC in carefully selected cases.

For comparison, information about the angular momentum (and its alignment) following DIC has also come from the angular distribution (1) of evaporated particles from the fragments, and (2) of the fission fragments when one DIC fragment subsequently fissions. In general these methods give somewhat higher alignments than derived above. Vandenbosch[17] derives $0.6 < P_{ZZ} < 0.8$ and Specht[18] finds $0.5 < P_{ZZ} < 1.0$ from fission studies. Ho et al.[19] find $P_{ZZ} < 0.8$ from α-particle evaporation. These results are probably not seriously inconsistent with the γ-ray value derived above, so that there is no clear discrepancy between the two types of data at the present time.

VI. Conclusion

I have tried to show that γ-ray studies have given information about the magnitude and the orientation of the angular momentum transferred in DIC. Although ambiguities can arise, it is possible to obtain reliable results provided the experimental conditions are carefully chosen. Under these circumstances, γ-ray methods can complete favorably with other methods available to obtain such information. Briefly we have learned from these studies about the time scale for equilibration of angular momentum into the internal degrees of freedom of the system, and that the equilibrium condition (in at least some cases) is a rigidly rotating composite system. However, when many l-waves and short time scales are involved, the angular momentum transfer becomes complicated. Further, we have learned that the DIC process introduces sizeable misalignments of the angular momentum when the Q-values are sufficiently large. It seems that all these features can be reproduced reasonably well by either classical dynamical models or transport models of DIC.

The potential of γ-ray methods to contribute further to DIC studies seems great. The present techniques are not yet fully developed, either for the resolved or the unresolved spectra. Other techniques, like total γ-ray energy measurements, are waiting to be tried. Perhaps most exciting, new 4π instruments are being developed which can measure the complete multiplicity, angular distribution, and total energy on an event-by-event basis. The possibility then exists of defining the spin and spin axis for each fragment in each event.

References

1. S. Cohen, F. Plasil, and W. J. Swaitecki, Ann. Phys. 81, 557 (1974).

2. R. S. Simon, M. V. Banaschik, J. O. Newton, R. M. Diamond, and F. S. Stephens, Phys. Rev. Lett. 36, 359 (1976).

3. J. B. Natowitz, M. N. Namboodiri, P. Kasiraj, R. Eggers, L. Adler, P. Gonthier, C. Cerruti, and T. Alleman, Phys. Rev. Lett. 40, 751 (1978).

4. M. A. Deleplanque, Th. Byrski, R. M. Diamond, H. Hubel, F. S. Stephens, B. Herskind, and R. Bauer, Phys. Rev. Lett. 41,, 1105 (1978).

5. M. Berlanger, M. A. Deleplanque, C. Gershel, F. Hanappe, M. LeBlanc, J. F. Mayault, C. Ngo, D. Paya, N. Perrin, J. Peter, B. Tamain, and L. Valentin, J. Phys. Lett. L37, 323 (1976).

6. P. Glassel, R. S. Simon, R. M. Diamond, R. C. Jared, I. Y. Lee, L. G. Moretto, J. O. Newton, R. Schmitt, and F. S. Stephens, Phys. Rev. Lett. 38, 331 (1977).

7. J. B. Natowitz, unpublished, from Ref. 3.

8. R. Regimbart, A. N. Behkami, G. L. Wozniak, R. P. Schmitt, J. S. Sventek, and L. G. Moretto, Phys. Rev. Lett. 41, 1355 (1978).

9. P. R. Christensen, F. Folkmann, Ole Hansen, O. Nathan, M. Troutner, F. Videbaek, S. Y. van der Werf, H. C. Britt, R. P. Chestnut, H. Freiesleben, F. Puhlhofer, Phys. Rev. Lett. 40, 1245 (1978).

10. A. Olmi, H. Sann, O. Pelte, Y. Eyal, A. Gobbi, W. Kohl, U. Lynen, G. Rudolf, H. Stelzer, and R. Bock, Phys. Rev. Lett. 41, 688 (1978).

11. G. Wolschin and W. Norenberg, Phys. Rev. Lett. 41, 691 (1978).

12. R. A. Dayras, R. G. Stokstad, C. B. Fulmer, D. C. Hensley, M. L. Halbert, R. L. Robinson, A. H. Snell, D. G. Sarantites, L. Westerberg, and J. H. Barber, Phys. Rev. Lett. 42, 697 (1979).

13. G. J. Woznaik, R. P. Schmitt, P. Glassel, R. C. Jared, G. Bizard, and L. G. Moretto, Phys. Rev. Lett. 40, 1436 (1978).

14. K. Van Bibber, R. Ledoux, S. G. Steadman, F. Videbaek, G. Young and C. Flaum, Phys. Rev. Lett. 38, 334 (1977).

15. H. Puchta, W. Dunnweber, W. Hering, C. Lauterbach, and W. Trautmann, Phys. Rev. Lett., to be published.

16. P. Aguer, G. J. Wozniak, R. P. Schmitt, D. Habs, R. M. Diamond, C. Ellegaard, D. L. Hillis, C. C. Hsu, G. J. Mathews, L. G. Moretto, G. U. Rattazzi, C. P. Roulet, and F. S. Stephens, submitted to Phys. Rev. Lett.

17. P. Dyer, R. J. Puigh, R. Vandenbosch, T. D. Thomas, and M. S. Zisman, Phys. Rev. Lett. 39, 392 (1977).

18. H. J. Specht, Proceedings of the Intern. Conf. on Nuclear Interactions, Australian Academy of Sciences, Canberra, Australia, Aug. 28-Sept. 2 (1978).

19. H. Ho, R. Albrecht, W. Dumweber, G. Graw, S. G. Steadman, J. P. Wurm, D. Disdier, V. Rauch, and F. Scheibling, Z. Physik A283, 234 (1977).

Figure Captions

Fig. 1. Schematic diagram of excitation energy vs spin in a nucleus around mass 160. The region of population following a DIC is indicated together with pathways for neutron evaporation and γ-ray deexcitation. The angular momentum at which the fission barrier vanishes is indicated, as are the entry and yrast lines.

Fig. 2. Unresolved γ-ray spectrum following the fusion reaction, $^{40}Ar + {}^{126}Te \rightarrow {}^{162}Yb^{*} + 4n$. Both the raw (open squares) and unfolded (corrected for response function, filled circles) spectra are shown. The variation with angular momentum input is shown at the bottom and the angular anisotropy at the top (Ref. 2).

Fig. 3. Systematics of the measured mean gamma multiplicity $\langle M_{\gamma} \rangle$ as a function of the average angular momentum of the compound nucleus, for various mass numbers (Ref. 3).

Fig. 4. Some systematics of the percentage of stretched E2 transitions observed following fusion reactions, as a function of neutron number of the principal product. The projectiles used in the fusion reaction are indicated (Ref. 4).

Fig. 5. Yield (top) and gamma-ray multiplicity (bottom) as a function of laboratory energy, for the system Cu + Au (Ref. 5).

Fig. 6. Gamma-ray multiplicity as a function of Z for the light product, following the reaction Ne + Ag. Data from three scattering angles are shown, as are the rolling and sticking limits for two values of the input angular momentum (Ref. 6).

Fig. 7. The mean angular momentum $\langle J \rangle_H$ of the heavy deep inelastic product is plotted as a function of its atomic number. The dashed curves correspond to the sticking prediction for different initial partial waves (here the two ions are assumed to be deformed at scission). Data are from Ref. 3.

Fig. 8. Gamma-ray multiplicities vs Z of the light fragment for the systems ^{86}Kr + $^{107,109}Ag$ and ^{86}Kr + ^{165}Ho. The solid points are for completely (energy) relaxed products, and the open points for partially relaxed products (Ref. 8).

Fig. 9. Gamma-ray multiplicity vs total kinetic energy for the systems ^{86}Kr plus $^{107,109}Ag$, ^{165}Ho, and ^{197}Au. Products whose light fragment had Z values between 30 and 39 were included (Ref. 8).

Fig. 10. (a) Schematic diagram of probability vs multiplicity for: exact distribution (top); first moment (middle); and first two moments (bottom). (b) A triangular angular-momentum input is illustrated, together with the first three moments of such a distribution.

Fig. 11. Values for the width, skewness, and anisotropy vs Z of the light product for the reaction ^{20}Ne + ^{63}Cu (Ref. 12).

Fig. 12. Schematic illustration of experimental arrangement (left) with beam, target, and detectors (position-sensitive parallel-plate counters), shown together with the resulting γ-ray angular distributions for stretched quadrupole (center) and dipole (right) transitions.

Fig. 13. Resolved γ-ray in-plane and out-of-plane relative yields are shown as a function of Q-value for transitions following the reaction $^{16}O + ^{27}Al$ (Ref. 14).

Fig. 14. The in-plane, out-of-plane anisotropies are shown at the top vs Q-value for the reaction $^{16}O + ^{48}Ti$. Resolved lines are shown as circles and unresolved regions of the γ-ray spectrum in coincidence with Z = 6 and 8 fragments are shown as squares. Center plot shows P_{ZZ} (Eq. (5)) for the initial ^{52}Cr fragment (resulting in ^{50}Cr after evaporating two neutrons), and the bottom plot shows the corresponding angular momentum input (Ref. 15).

Fig. 15. The out-of-plane (left) and in-plane (right) angular anisotropy for the symmetric products ($A \approx 160$) from the reaction $^{136}Xe + ^{197}Au$, as a function of γ-ray energy. Three different Q-value regions are shown (Ref. 16).

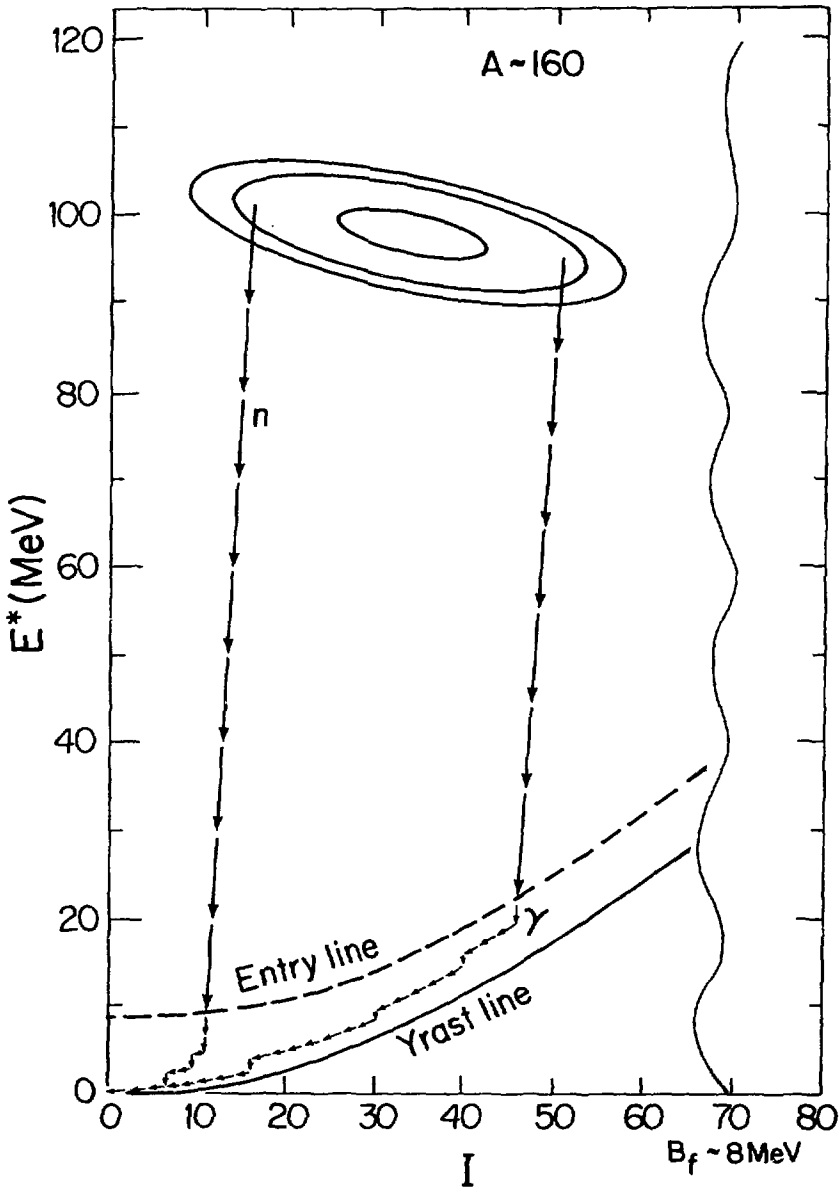

XBL 7912 - 13378

Fig. 1

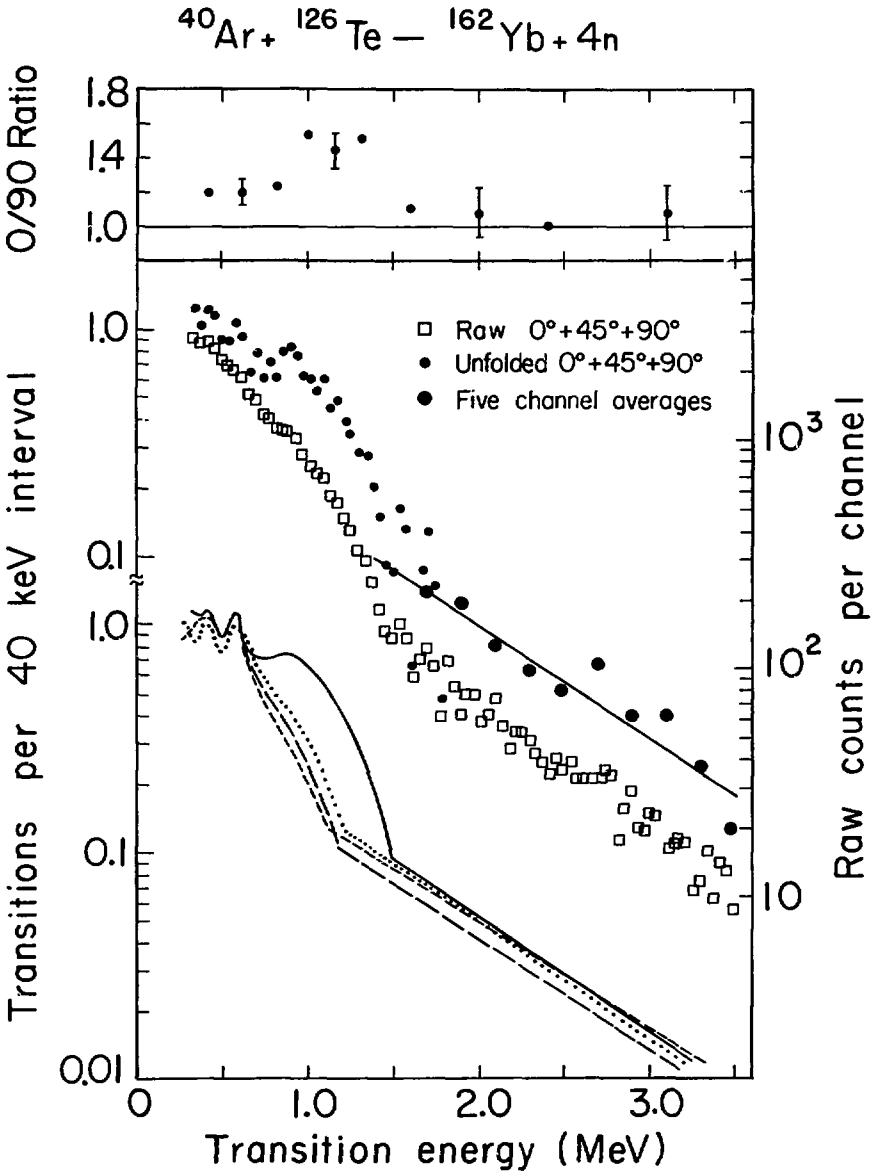

XBL 771-162

Fig. 2

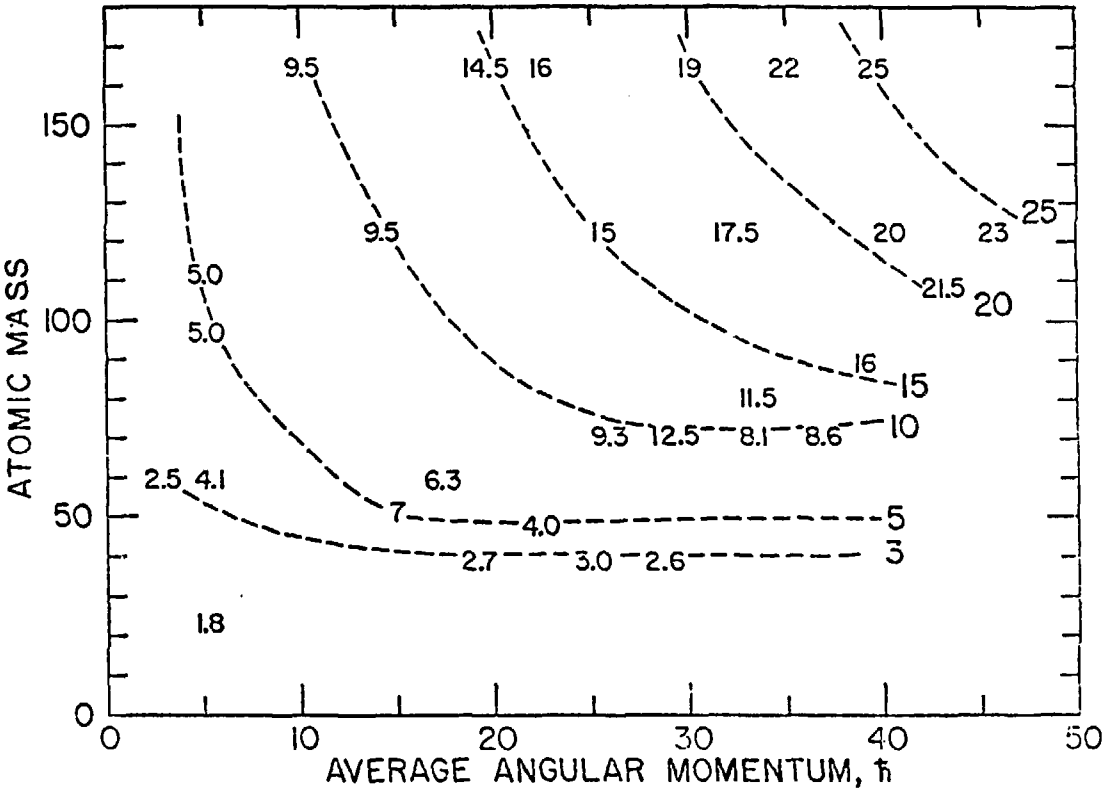

XBL 7912-13679

Fig. 3

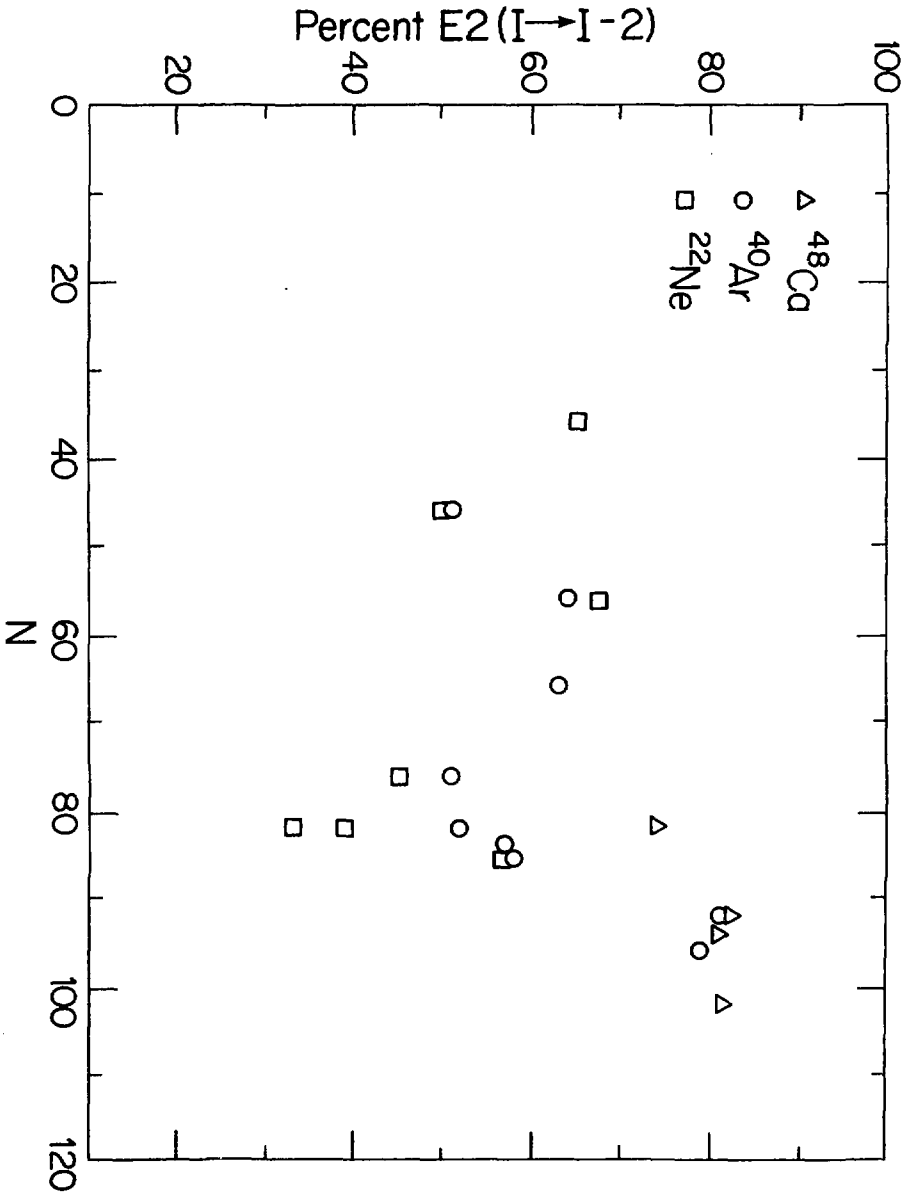

XBL 7912-13379

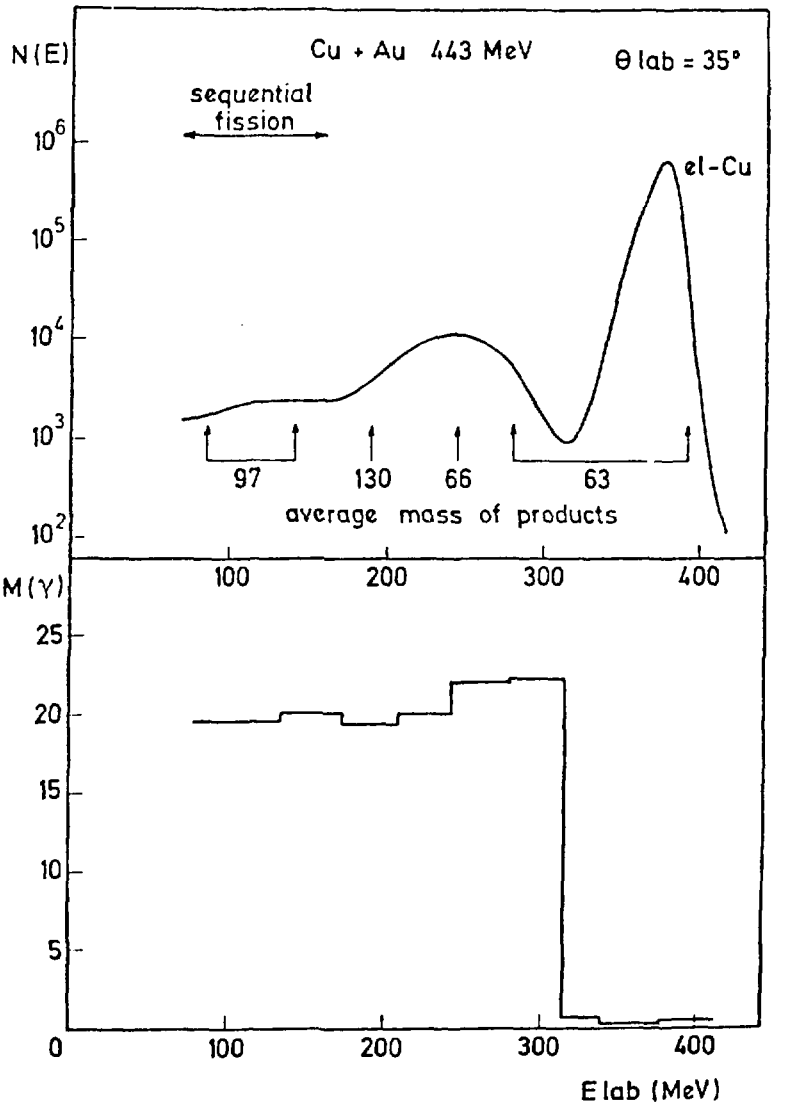

XBL 7912-13681

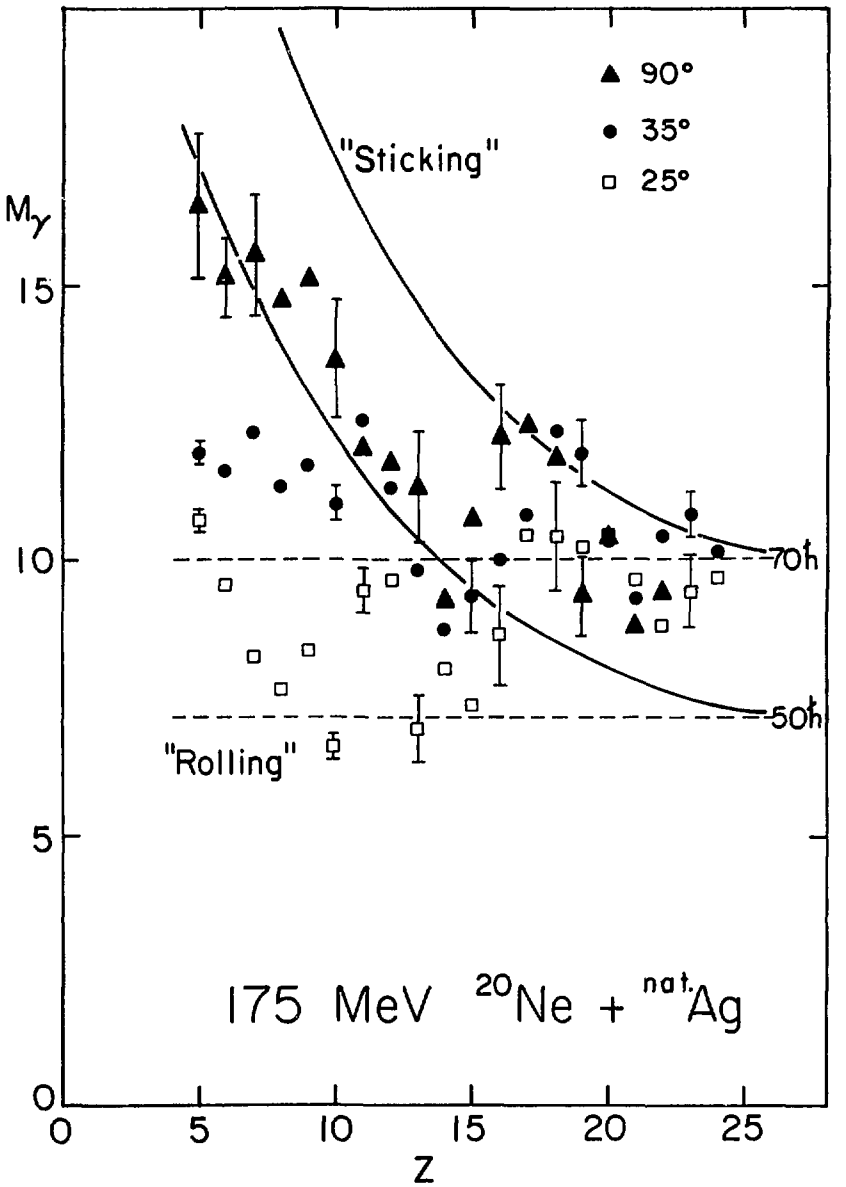

XBL7611-4446

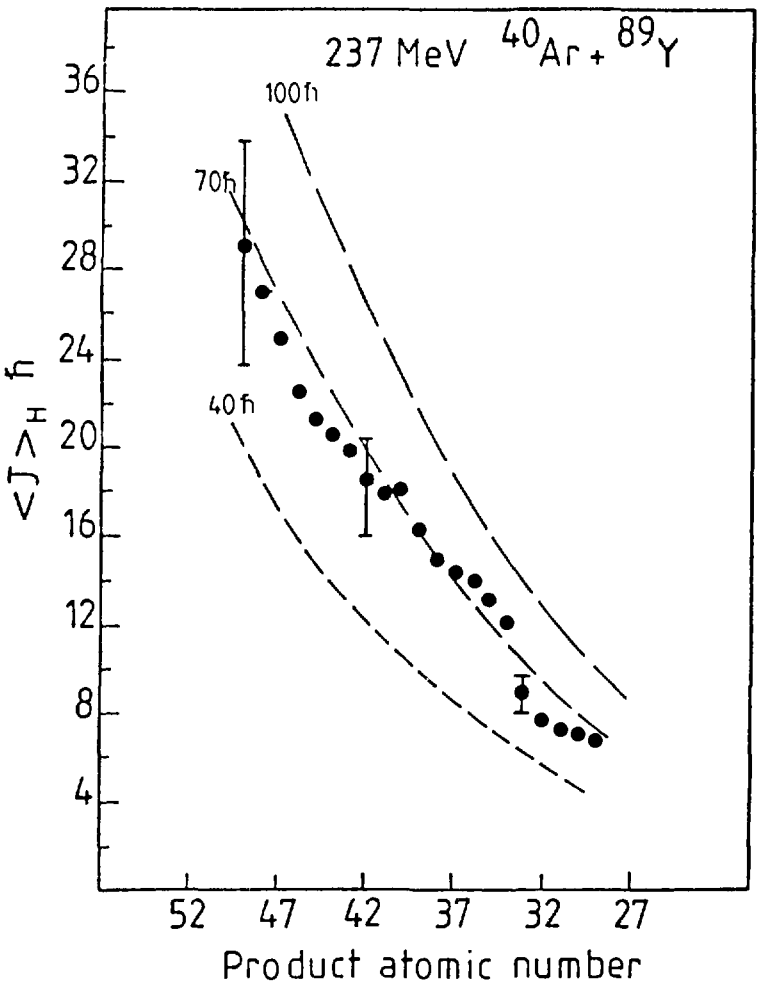

XBL 7912-13683

Fig. 7

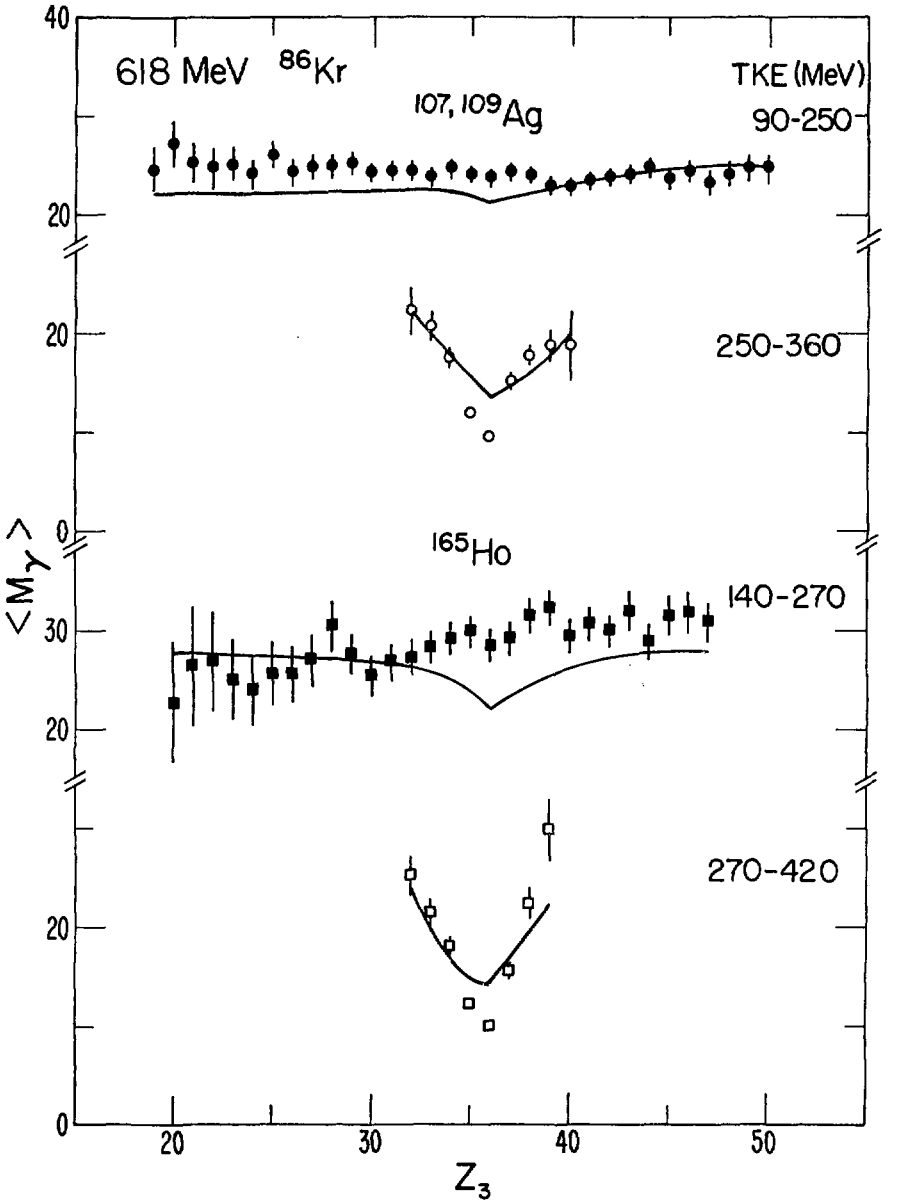

XBL 786-2556

Fig. 8

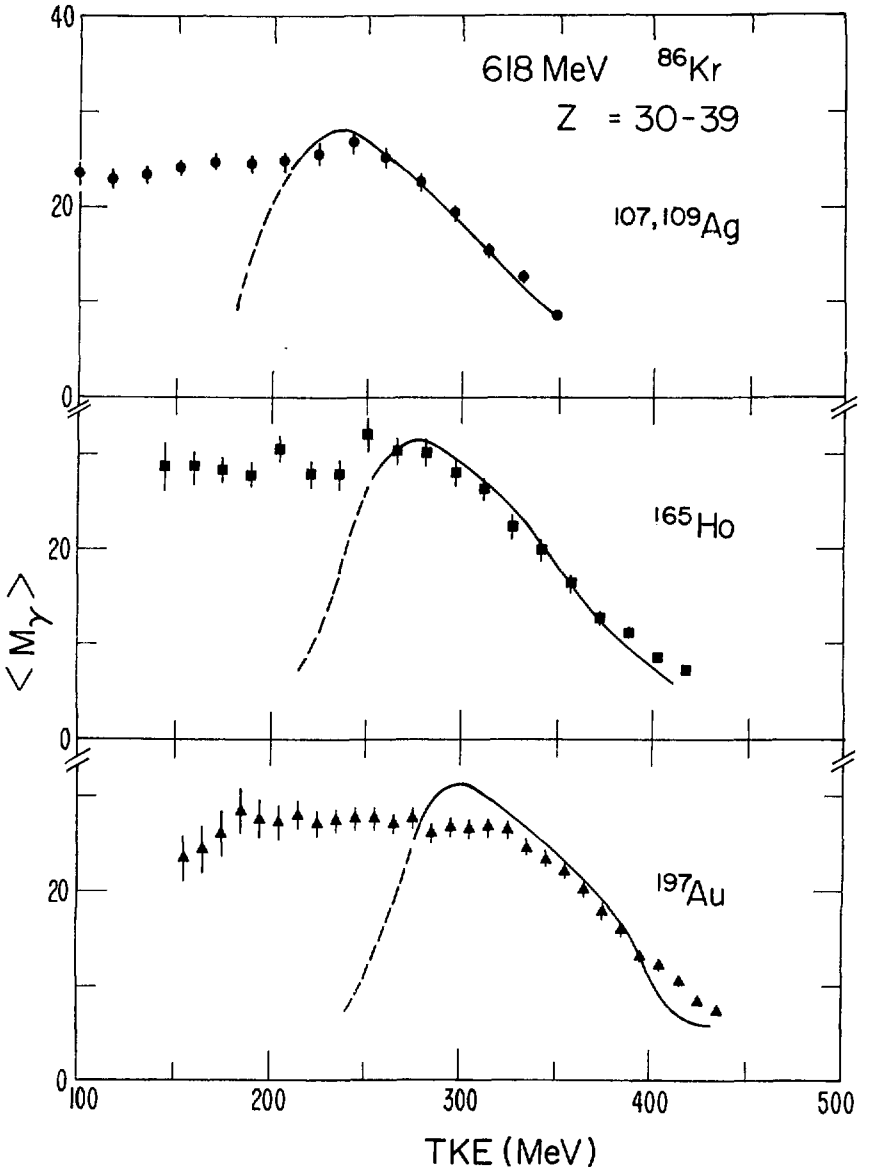
618 MeV ^{86}Kr
Z = 30-39
^{107,109}Ag
^{165}Ho
^{197}Au
$\langle M_\gamma \rangle$
TKE (MeV)
0
20
40
100
200
300
400
500

XBL 786-2553

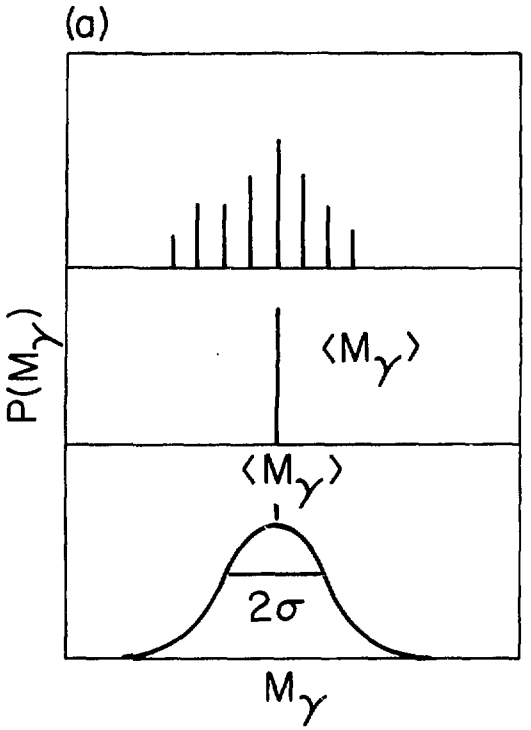

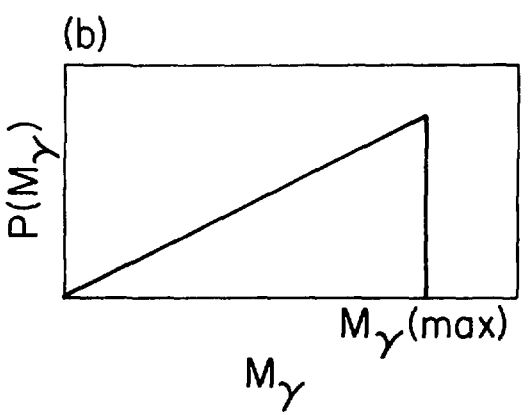

$\langle M_\gamma \rangle =$
$2/3\ M_\gamma(\max)$
$\sigma / M_\gamma = 0.35$
$s = -0.57$

XBL 7912 - 13381

Fig. 10

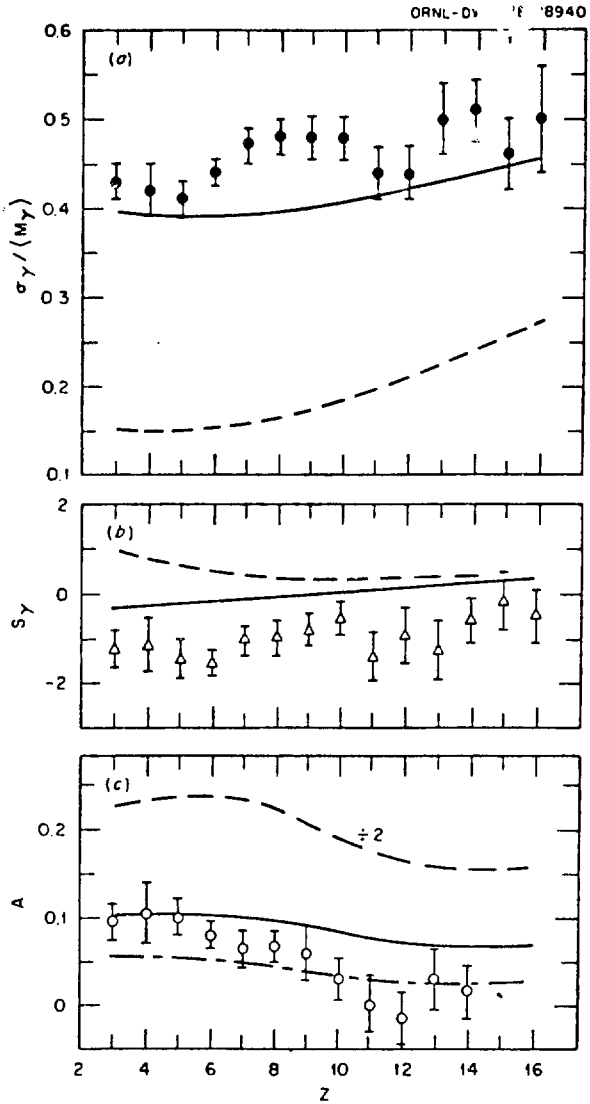

XBL 7912-13682

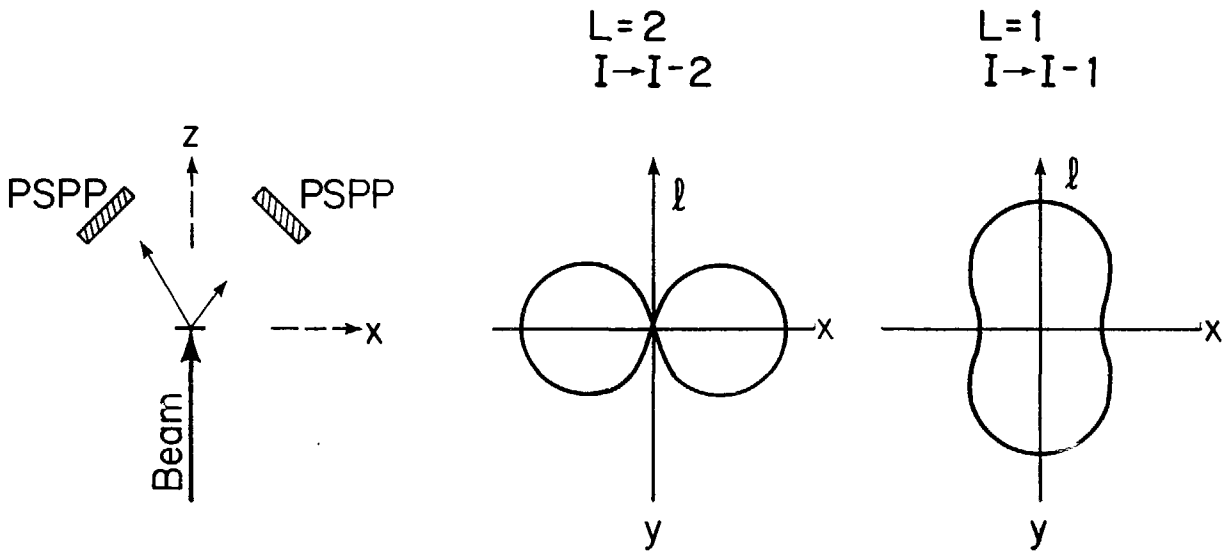

XBL 7912 - 13380

Fig. 12

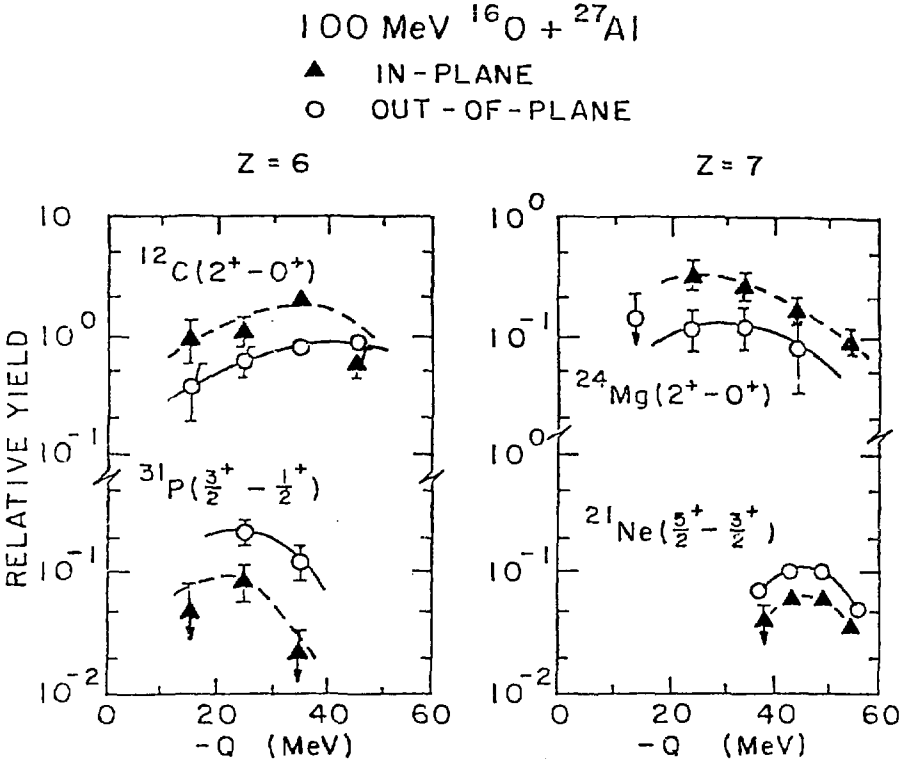

	$\frac{W(\text{IN-PLANE})}{W(\text{OUT-OF-PLANE})}$	
	EXP.	CALC. (FULL ALIGNMENT)
$^{24}Mg\,(2^+-0^+)$	2 - 3	2.4
$^{21}Ne\,(\frac{5}{2}^+ - \frac{3}{2}^+)$	~0.5	0.5

XBL 7912-13680

Fig. 12

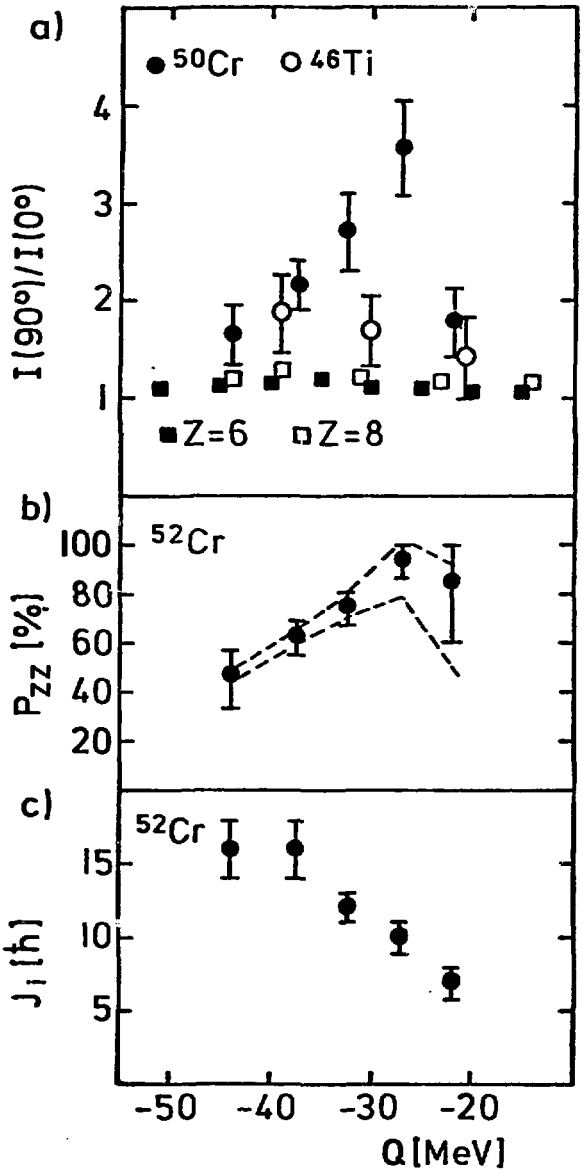

XBL 7912-13678

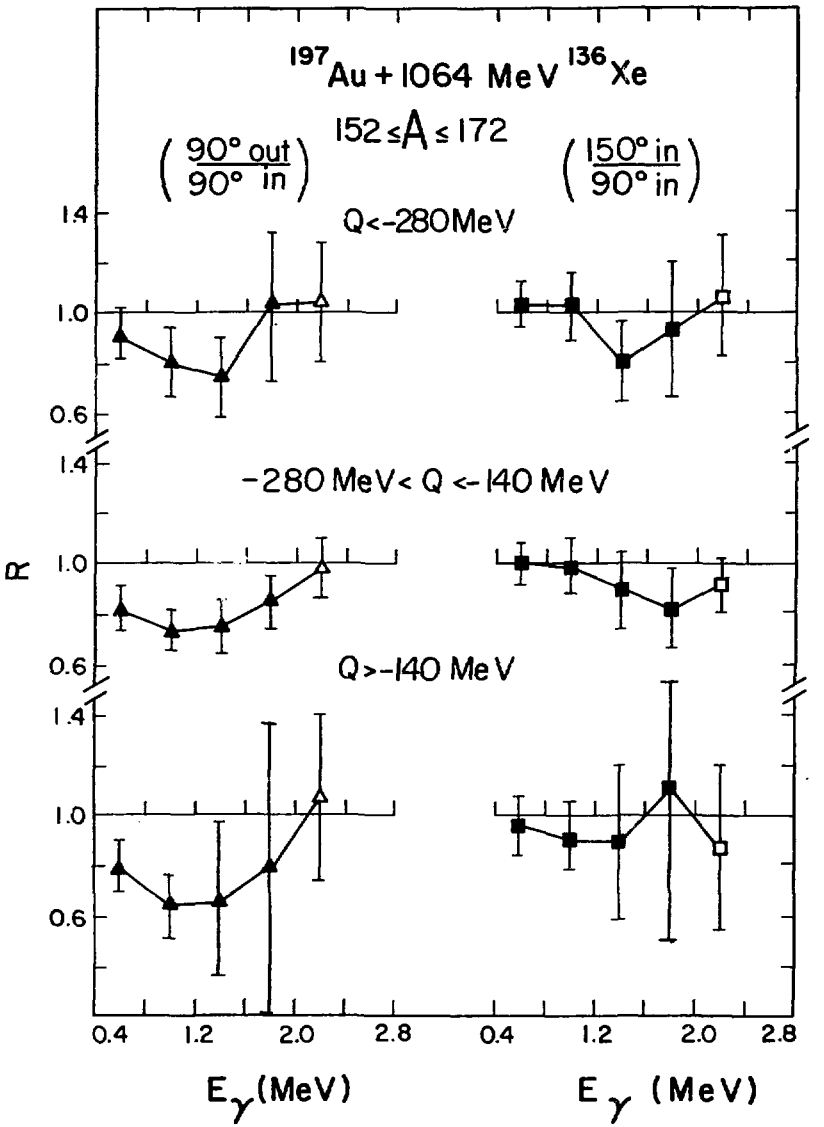
197Au + 1064 MeV 136Xe
152 ≤ A ≤ 172
(90° out / 90° in)
(150° in / 90° in)
Q<-280MeV
-280 MeV< Q <-140 MeV
Q>-140 MeV
R
1.4
1.0
0.6
0.4
1.2
2.0
2.8
Eγ(MeV)
Eγ (MeV)

XBL 797-2298